Published in final edited form as:
J Mol Cell Cardiol. 2015 February ; 79: 69–78. doi:10.1016/j.yjmcc.2014.10.011.

Ca^{2+} Sparks and Ca^{2+} Waves are the subcellular events underlying Ca^{2+} overload during ischemia and reperfusion in perfused intact hearts

Mattiazzi Alicia[1], **Argenziano Mariana**[2,3], **Aguilar-Sanchez Yuriana**[3], **Mazzocchi Gabriela**[1], and **L. Escobar Ariel**[3]

[1]Centro de Investigaciones Cardiovasculares, CONICET-La Plata, Facultad de Medicina, UNLP, Argentina

[2]Universidad Nacional de San Martin, San Martin, Argentina

[3]Biological Engineering and Small Scale Technologies, School of Engineering, University of California, Merced, CA, USA

Abstract

Abnormal intracellular Ca^{2+} cycling plays a key role in cardiac dysfunction, particularly during the setting of ischemia/reperfusion (I/R). During ischemia there is an increase in cytosolic and sarcoplasmic reticulum (SR) Ca^{2+}. At the onset of reperfusion there is a transient and abrupt increase in cytosolic Ca^{2+} which occurs timely associated with reperfusion arrhythmias. However, little is known about the subcellular dynamics of Ca^{2+} increase during I/R and a possible role of the SR as a mechanism underlying this increase has been previously overlooked. The aim of the present work is to test two main hypotheses: 1. An increase in the frequency of diastolic Ca^{2+} sparks (cspf) constitutes a mayor substrate for the ischemia-induced diastolic Ca^{2+} increase; 2. An increase in cytosolic Ca^{2+} pro-arrhythmogenic events (Ca^{2+} waves), mediates the abrupt diastolic Ca^{2+} rise at the onset of reperfusion. We used confocal microscopy on mouse intact hearts loaded with Fluo-4. Hearts were submitted to global I/R (12/30 min) to assess epicardial Ca^{2+} sparks in the whole heart. Intact heart sparks were faster than in isolated myocytes whereas cspf was not different. During ischemia, cspf significantly increased relative to preischemia (2.07±0.33 vs. 1.13±0.20 sp/sec/100μm, n=29/34, 7 hearts). Reperfusion significantly changed Ca^{2+} sparks kinetics, by prolonging Ca^{2+} sparks rise time and decreased cspf. However it significantly increased Ca^{2+} wave frequency relative to ischemia (0.71±0.14 vs. 0.38±0.06 w/sec/100μm, n=32/33, 7 hearts). The results show for the first time the assessment of intact perfused heart Ca^{2+}

Correspondence to: Dr. Ariel L. Escobar, Biological Engineering and Small Scale Technologies, School of Engineering, University of California, Merced, CA, USA. Phone: 209-216-4616, Fax:209-216-4108, aescobar4@ucmerced.edu.

Disclosures
None.

sparks and provides direct evidence of increased Ca^{2+} sparks in ischemia that transform into Ca^{2+} waves during reperfusion. These waves may constitute a main trigger of reperfusion arrhythmias.

Introduction

Ischemic heart disease is invariably characterized by impaired cardiac function and disturbed Ca^{2+} homeostasis. Regardless of its accepted clinical significance, our understanding of the subcellular mechanisms of myocardial ischemia reperfusion (I/R) injury is still limited. Indeed, there is a big gap in knowledge between the severity of the myocardial I/R process and the intracellular Ca^{2+} dynamics. Different laboratories including our own, have shown an increase in diastolic Ca^{2+} during ischemia [1–4], which has been associated with a rise in Na^+ [5,6]. The increase in intracellular Na^+ has been attributed to a decrease in Na^+ extrusion due to several concurrent factors like the inhibition of the Na^+/K^+-ATPase, the increase in Na^+ influx through the Na^+/H^+-exchanger (NHE) and Na^+-$HCO3^-$ cotransporter [7,8], and the persistent Na^+ current [9]. Additional Na^+-independent sources of cytosolic Ca^{2+} increase during ischemia have also been suggested to participate. For instance, an increase of the influx of Ca^{2+} through the L-type Ca^{2+} channels [10] or the impaired activity of the sarcoplasmic reticulum (SR) Ca^{2+}-ATPase (SERCA) due to the low ATP concentrations reached during ischemia [11,12] promote an elevated cytosolic Ca^{2+}. Although this later effect might anticipate a Ca^{2+}-unloaded SR during ischemia, experiments from our laboratory, in perfused intact heart, revealed that SR Ca^{2+} actually increases in parallel with cytosolic Ca^{2+} [4].

It has long been known that SR Ca^{2+} release can occur spontaneously under conditions of SR Ca^{2+} overload in the absence of membrane depolarizations [13,14]. Thus, ischemia should be added to the list of conditions that, like excessive β-adrenergic stimulation, Na^+ overload, elevated extracellular Ca^{2+} concentrations, or fast pacing, can trigger spontaneous SR Ca^{2+} release. However, a possible involvement of SR in ischemia-induced cytosolic Ca^{2+} increase has been systematically overlooked. Moreover, little is known about the dynamics of the subcellular mechanisms underlying Ca^{2+} increase during ischemia and reperfusion. The first hypothesis be tested in this work is that an increase in the frequency of diastolic Ca^{2+} sparks constitutes a mayor substrate for the increase in diastolic Ca^{2+} during ischemia. Ca^{2+} sparks are subcellular events that condition both, the diastolic Ca^{2+} concentrations and the SR Ca^{2+} load. Although sparks have been extensively characterized in isolated cells at room temperature, the behavior of these random microscopic events is unclear at the intact heart level and at temperatures close to the physiological range for mammalian function. Accordingly, it is a must to evaluate the kinetics and likelihood of Ca^{2+} sparks in the intact heart to fully understand the basis of Ca^{2+} mishandling during ischemia and reperfusion.

At the onset of reperfusion there is also a transient increase in cytosolic Ca^{2+} which has been related to reperfusion arrhythmias. Although this increase has been usually associated with an influx of Ca^{2+} from the extracellular space [15,16], we recently showed experiments performed at the epicardial (epi) layer of the heart in which there is an abrupt and massive increase in cytosolic Ca^{2+} promoted by Ca^{2+} released from the SR [4]. Yet, it is unknown

whether this Ca^{2+} release gives rise to proarrhythmogenic Ca^{2+} waves. The second hypothesis to be evaluated in this work is that the abrupt diastolic Ca^{2+} rise at early times during reperfusion is mediated by an increase in cytosolic Ca^{2+} proarrhythmogenic events (i.e. Ca^{2+} waves). To test the two main hypotheses stated above, we evaluated Ca^{2+} sparks and waves at the epi layer of a perfused mouse heart loaded with the Ca^{2+} indicator Fluo-4. The subcellular Ca^{2+} dynamic was assessed by spectroscopic measurements on an upright confocal microscope in the setting of I/R.

Since myocardial I/R is a major cause of left ventricular dysfunction and lethal arrhythmias, knowledge of the subcellular events underlying these alterations has potential broad implications for cardiovascular medicine.

Methods

Heart Preparation

Animals used in this study (male C57 mice of 3–7 weeks-old) were maintained in accordance with the National Institutes of Health Guide for the Care and Use of Laboratory Animals (NIH Publication No. 85–23, Revised 1996) and were euthanized by cervical dislocation. This protocol was approved by the Merced Institutional Animal Care and Use Committee of the University of California Merced (# 2008–201). After removing hearts from the mice, the aorta was cannulated and connected to a custom design recording chamber attached to a Langendorff apparatus for constant perfusion. Sinoatrial node was dissected for all the hearts and atrioventricular node was mechanically impaired to gain external pace control in electrophysiological and Pulsed Local Field Fluorescence Microscopy (PLFFM) measurements (see below). The recording chamber was positioned under a stereoscopic microscope located just beside the upright confocal microscope (Fluoview 1000, Olympus, Japan), which was used for the spark and waves recordings. Hearts were perfused with normal Tyrode solution (in mmol/L: 2 $CaCl_2$, 140 NaCl, 5.4 KCl, 1 $MgCl_2$, 0.33 Na_2HPO_4, 10 HEPES, 10 glucose, pH 7.4). The temperature of the solution outside the heart was controlled with a Peltier unit that allowed us to maintain the heart temperature within a narrow range during the whole experiment. All solutions were equilibrated with 100% O_2.

Fluorophore Loading

Fluo-4 AM or Rhod-2 (for PLFFM experiments) (Invitrogen, Carlsbad, CA, USA) were used to measure changes in the myoplasmic Ca^{2+} concentration. The dyes were dissolved in 45–60 μL DMSO (Sigma, St Louis, MO, USA) with 2.5% Pluronic and added to 1 mL normal Tyrode solution. Perfusion with dyes started after the spontaneous heart rate became regular (within 10 min after cannulation). After 45 min of perfusion at room temperature (21–23°C), the solution was switched to normal Tyrode and the temperature was increased to 32°C within 10 min. Then, the recording chamber was positioned on the stage of the confocal microscope.

Confocal Optical Recordings

A modified upright confocal microscope with a very long working distance and high numerical aperture (0.95) 20 X objective, was used for the fluorescence recordings. Both line scan recordings and 2D images were obtained from the left ventricular epi layer. The point spread function of the system (obtained as the impulse response to a 60 nm fluorescent bead and a pinhole aperture of 75 μm) reflects a half width of 0.62 μm and a depth of field of 1.45 μm. A combination of gravity plus peristaltic recirculation was used to maintain the heart under quasi physiological conditions. The heart was maintained immersed in the recording solution for the time course of the experiment to facilitate focus through the water immersion objective. An important difficulty of recording spark activity in an intact heart is the endogenous electrical activity of the organ and the movement artifacts. The electrical activity was impaired by using a combination of 15 μmol/L of Tetrodotoxin (TTX, Alomone, Israel) to block $Na_v1.5$ sodium channels and 6 μmol/L of carbamylcholine (Sigma, St Louis, MO, USA) to induce a deep bradycardia (~2 beats/min). During the confocal recordings the hearts were not externally paced. Additionally, cardiac contraction was prevented by the use of 5 μmol/L of the mechanical uncoupler, blebbistatin (Sigma, St Louis, MO, USA), that blocks actin-myosin interaction and cross bridge cycling [17], and a small pin was introduced in the apex of the left ventricle and fixed to the chamber to minimize lateral movements. The temperature of the heart and the flow rate were controlled during the experiment. In some experiments, Fluo-4 PLFFM was used to record intracellular Ca^{2+} transients in intact paced hearts at different temperatures (See Figure 3 supplementary material).

In the intact heart the likelihood of getting Ca^{2+} sparks is rather low. In a whole heart frame, we usually have 25 to 40 cells and most of these frames have no sparks. Moreover, due to the tissue curvature, only a fraction of the field will be in focus with respect to the total field. To made a systematic analysis of Ca^{2+} sparks in the intact heart that allows comparison among the different situations studied (See below), we carefully scanned the epi layer of the heart and stopped in when a sparking cell was found. Line scan recordings were obtained for sparking cells. The spark frequency was calculated as the number of sparks per 100 μm per second ($Spark\ Frequency = \frac{\#\ of\ Sparks}{100\ \mu m * 1s}$.)

Whole heart electrophysiological measurements

Transmembrane action potentials (APs) were recorded with glass microelectrodes as previously described [18]. Half duration of action potential (APD) of phase 2 were utilized to assess the degree of ischemia.

Ischemia and reperfusion protocols

After stabilization (preischemia), hearts were subjected to 12 min global ischemia. At the end of ischemia, constant coronary flow perfusion was restored for 30 min (reperfusion). This protocol was chosen based on the results of previous experiments which indicate that this ischemic period produced reversibly altered APs, Ca^{2+} handling and mechanical dysfunction, typical of the stunned heart [19]. Figure 1A of supplemental data shows typical recordings of AP modifications during the applied I/R protocol. There is a significant

shortening of APs that stabilizes between 8 and 12 min of ischemia and then recovers during the reperfusion period. Figure 1B of supplemental data shows the statistics of 6 experiments. Optical recordings were obtained every 3 min during preischemia, ischemia and reperfusion.

Isolated myocyte experiments

Ventricular myocytes were enzymatically isolated as previously described[18]. After dissociation, cells were loaded (60 min, room temperature) with the acetoxymethyl ester (AM) form of Fluo-4. Indicator loaded cells were rinsed continuously for 15 min before use. The recordings were obtained at 32°C to mimic the conditions used in the intact heart.

Pulsed Local Field Measurements

PLFFM that was used for determining the epi and endocardial (endo) Ca^{2+} transients[20]. Briefly, the exciting green light source (532 nm) Yag laser was focused by a standard microscope objective (40x, NA 0.45) into a small (200 μm dia) multimode optical fiber for transmission of the exciting light to the epi and/or endo layers. Optical fibers to record endo signals were introduced in the left ventricular chamber with the aid of an intravitral surgery sclerotomy adaptor (Alcon, USA). Emitted light is carried back through the same fiber, filtered to eliminate the reflected excitation component, and focused on an avalanche photodiode that is connected to an integrating current-to-voltage (I–V) converter controlled by a digital signal processor (DSP). Fluorescence signals were digitized at a sampling frequency of 500 kHz and a bandwidth of 125 kHz. The acquisition system was controlled by a PC running a custom-designed, G-based software program (LabVIEW). The recordings were obtained by gently placing one end of the fiber on the tissue. Hearts were continuously paced at different heart rates at 32°C.

RTPCR

Left ventricle slicing—Hearts were removed from mice (male, age: 3–7 wk old). The aorta was cannulated and connected to a horizontal Langendorff apparatus for constant perfusion with normal Tyrode solution. After the blood was removed from the coronary circulation, the hearts were perfused with an RNA*later* (Qiagen) solution in order to inhibit the RNAses and preserve the structure of the tissue. Ventricles were removed and maintained at 4°C. Square pieces of 4 by 4 mm were included in a low melting point agarose solution to facilitate the slicing. The included specimens were positioned, half placed with Epi on top and half with Endo on top, in the stage of a vibratomic slicer (Leica VT1000S, Leica inc) and sliced with a thickness of 200 μm. The first slice was always eliminated, whereas the subsequent two slices were preserved for mRNA measurements. Slices were maintained at 4°C until the experiments were performed.

RNA extraction: individual slices were placed in a 0.5 ml Eppendorf containing 1ml of Trizol Reagent. Tissue was homogenized with the aid of an ultrasonic cell disruptor. The homogenate was incubated for 5 min at room temperature and 0.2ml of chloroform per ml of Trizol was added. After 2–3 min of incubation, the sample was centrifuged at 12000g 15 min 4°C. The supernatant was removed and 1ml of 75% ethanol per ml of Trizol was added and centrifuged at 7500g for 5 min at 4°C. After the supernatant was removed, the sample was dried for 15–30min and the pellet dissolved in 30μl of RNAse free water.

Reverse Transcription—RNA was be quantified by using the Nanodrop and 2 μg was used for the reverse transcription reaction. 2μg of RNA was mixed with 1μl of Random primers (200ng/μl) and RNAse free water up to 12.5 μl. 7.5 μl of a MIX solution containing 4μl of reaction buffer, 0.5 μl of RNAse free water, 2 μl dNTPs mix and 1μl of RevertAid was added before the thermocycle cycles began. cDNA obtained was stored at −80°C.

Real-Time PCR—cDNA samples were diluted with RNAse free water and 6.25 μl of Mix (FastStart Roche), 4.5μl of water (RNAse free), 0.37μl of forward primer, 0.37 μl of reverse primer were added. The tubes were placed in a plate and RT PCR cycles were started. Finally, Gapdh was used as a housekeeping gene.

Data Analysis

Ca^{2+} sparks were analyzed in Image J using the sparkmaster plugin. Time to peak and half duration histograms were computed and Log binned time distributions were computed [20]. Arithmetic moments of the distributions were calculated with parameters obtained by fitting the histograms with a log normal distribution. Spark and wave frequency was estimated by counting the number of sparks during the entire recording and expressed as number of events/s normalized to 100 μm. Wave velocity was calculated from the slope of line scan image and expressed in μm/s. A propagated Ca^{2+} wave was defined as a continuous wave-front in the line scan image visualized as a robust fluorescent line that propagates across the full width of the myocyte without breaking down into sparks. Statistical significance was tested using ANOVA. Differences were considered to be significant if P values were less than 0.05.

Results

In previous papers [4,19], we demonstrated that diastolic and systolic Ca^{2+} increased during ischemia in association with a decrease in Ca^{2+} transient amplitude. We also showed that there was a further abrupt increase in cytosolic Ca^{2+} at the onset of reperfusion, which was released from the SR [4]. To study the subcellular mechanisms underlying the increase in Ca^{2+} during I/R, we used confocal microscopy in the intact heart.

Epi Ca^{2+} sparks in the intact hearts

Figure 1A is an example of a line-scan-recording of epi Ca^{2+} sparks obtained in the intact heart. Figure 1B shows the kinetic features of epi Ca^{2+} sparks activation. As it is possible to expect, the distribution of the time to peak of Ca^{2+} sparks follows an exponential behavior due to the relationship that exists between the mean open time of the RyR2 and the time to peak of Ca^{2+} sparks. However, when the data expands over several orders of magnitude, a log representation for time distribution is more suitable because reduce the errors in estimating fitted parameters in comparison with linear finite sampling intervals and binning [21,22]. Thus Figure 1C, represents the logarithm binned histogram where the asymmetric bell shape distribution of the logarithmic time to peak is consistent with the exponential conduct of the process and allowed us to evaluate the expectation of the time to peak of Ca^{2+} spark distribution (tp=9.5 ±0.3 ms). A summary of these results is shown is Fig. 1F where an x-t plot of an average of 10 sparks is presented.

Epi whole heart Ca^{2+} sparks display unusually fast kinetics, being significantly faster than the ones reported in other cardiac models like trabeculae [23]. Interestingly, these epi whole heart Ca^{2+} sparks also have a distribution of the durations at half maximum that is shifted to shorter sparks durations (Figure 1D) (FDHM= 28.5 ±0.2 ms). In contrast, their spatial spreading look wider (Figure 1E) (FWHM= 3.0 ±0.1 μm) than the ones reported in rat cardiac trabeculae under comparable experimental conditions [23]. These kinetic differences could be interpreted as differences in the kinetic properties of Ca^{2+} signaling between epi and endo tissue. To evaluate this idea, we performed experiments to simultaneously measure Ca^{2+} transients from the epi and endo layer of an intact perfused heart by means of PLFFM. Typical fluorescence recordings of epi and endo transients are illustrated in Fig. 2A. Activation is slower and the half duration longer for Ca^{2+} transients recorded in endo than in epi. A comparison of the activation rise times and time to peaks are shown in Fig. 2B. Both parameters are significantly slower in endo than in epi (n= 6 animals).

Experiments presented in Fig. 2A and B revealed the functional differences of Ca^{2+} transients across the ventricular wall. However, they do not provide any molecular explanation for these differences. This molecular piece of information was obtained by measuring the mRNA levels in vibrotomically cut epi and endo left ventricular slices (200 μm). Total RNA was obtained from mice (n=5) and reverse transcription was carried out using random primers and reverse transcriptases (Fermentas). mRNAs levels were normalized to Gapdh mRNA and analyzed by the Pfaffl method, an Epi and Endo comparison is shown in Fig. 2C. The analysis tells that the faster activation and relaxation of Epi Ca^{2+} transients have a high correlation with higher mRNA levels for RyR2 and SERCA2a. As we expected, the mRNA levels for Kv 4.3 are higher in epi than in endo. This nicely correlates with a higher density of Ito, responsible of AP phase 1 in epi [24,25].

Comparison between Ca^{2+} sparks in intact heart vs. isolated myocytes

Additionally, our results also revealed that epi Ca^{2+} sparks in the intact heart are faster than those observed in isolated cells [26,27]. However, it is difficult to discern if the more rapid raise and relaxation of these diastolic stochastic events in the intact heart vs. isolated cells is due to either different preparations properties or different experimental conditions like the temperature at which the experiments were performed. As far as we know, this is the first report of Ca^{2+} sparks in an intact heart. Therefore, we think it is appropriate, although it is not the main focus of this paper, to compare the time course and spatial properties of whole heart Ca^{2+} sparks with those observed in isolated cells. To address this issue, we performed experiments in isolated ventricular myocytes at the same temperature and under the same experimental conditions (i.e. same dye concentration and incubation/perfusion time, recording chamber, confocal microscope, pinhole diameter, temperature, etc.) like those used in the intact heart. Experiments shown in Figure 3 summarize the central kinetic and spatial findings of single myocytes Ca^{2+} sparks recorded at 32°C. Figure 3A illustrates line scan recordings of Ca^{2+} sparks at 32°C. Evaluation of the spatial profile of Ca^{2+} sparks recorded in isolated myocytes under these experimental conditions indicates that the full width half maximum is significantly smaller than the ones recorded at the epicardium (FWHM= 2.24 ±0.05 μm) (Figure 3D). However, the two most striking differences, between whole heart epicardium and isolated ventricular myocyte Ca^{2+} sparks, are the rates of

activation and relaxation. Indeed, as shown in Figure 3B, the time to peak was increased two folds (Tp= 18.91 ±0.24 ms). Moreover, the rate of relaxation increased dramatically in isolated myocytes and the distribution of the durations at half maximum were also shifted to almost double (FDHM= 51.40 ±0.4 ms) (Figure 3C) in comparison with the whole heart measurements. These results indicate that the kinetic differences between whole heart epicardium and isolated ventricular myocytes seem not to arise from the different experimental conditions used in the different experiments. Another possible cause of the disparity of the results between isolated cells and the whole heart may lie in the resulting mix of myocytes obtained during the isolation process from different layers (i.e. epicardium, midmyocardium and endocardium). Thus, it is also possible to postulate that different ventricular layers display dissimilar microscopic Ca^{2+} dynamics, as discussed above. Moreover, the kinetic differences may be also produced by differences in the SR Ca^{2+} loading. Actually, increases in the Ca^{2+} load at the whole heart level produce increases in both, time to peak and half duration of Ca^{2+} transients induced by AP depolarization [28]. Besides the kinetic and spatial extension differences between whole heart epicardium and isolated myocytes, there are other critical parameters that define the impact of Ca^{2+} sparks on the diastolic Ca^{2+} regulation. Unfortunately, a comparison between the distributions of Ca^{2+} sparks between whole heart and isolated cells presents several challenges that at this stage are not possible to overcome. Ca^{2+} spark measurements as ΔF/F0 at the whole heart level are highly influenced by the much higher nonspecific resting fluorescence of the organ. Moreover, a Ca^{2+} sparks parameter that is possible to quantify both, in the intact preparation and isolated cell, is the frequency of Ca^{2+} sparks. However, it is not possible to determine if the frequency of sparks in cells that are sparking is significantly different between both preparations. In isolated cell experiments, cells are lying flat at the bottom of the chamber, while at the epicardium, a smaller fraction of the field is in focus with respect to the total field, due to the high curvature of the tissue. This factor prevents us to compare isolated cells vs intact tissue. Nevertheless as in the intact heart experiments, we always have the same geometric curvature between preischemia, ischemia and reperfusion, a quantitative comparison between these conditions can be performed. A summary of the comparison between spark properties for both preparations is presented in Figure 3E–G.

Subcellular Ca^{2+} dynamics during ischemia and reperfusion

Ischemia does not modify the kinetic properties of Ca^{2+} sparks but does increase the likelihood of Ca^{2+} sparks—It has already been shown that ischemia induces an increase in cytosolic Ca^{2+} [4,19]. Although several mechanisms have been proposed to explain this Ca^{2+} increase, a possible role of spontaneous Ca^{2+} release from the SR has not been previously explored. To further study the nature of the subcellular mechanisms involved in the ischemia-induced increase in Ca^{2+}, we performed confocal measurements of the subcellular Ca^{2+} dynamics. Specifically, the flow was interrupted and the epi layer was refocused due to the positional change induced by the procedure. Line scan recordings were obtained from 2 min after the ischemia was initiated to the end of the ischemic insult (12 min). The validity of this protocol was evaluated in independent experiments where the half duration of epi AP phase 2 was used as a metric of the degree of challenge induced by the ischemic insult (Figure S1 of supplementary material).

Although, none of the kinetic and spatial parameters of Ca^{2+} sparks were modified during the insult (Fig 4A–D), the frequency and the number of cells presenting Ca^{2+} sparks were significantly increased with respect to preischemia (see Figure 6D).

Ca^{2+} sparks are not the only spontaneous events underlying intracellular Ca^{2+} dynamics during ischemia. Under conditions in which the SR Ca^{2+} load is increased, Ca^{2+} sparks can trigger Ca^{2+} waves. Interestingly, the frequency and the velocity of Ca^{2+} waves did not increase during the ischemic insult. Data supporting this last statement are presented in Fig 4E–G, where the spatial profile and velocities are shown for both, the preischemic and the ischemic conditions. In contrast, common events observed in association with the frequent Ca^{2+} sparks during ischemia are non-propagated mini-waves or wavelets, similar to those observed with antiarrhythmic agents like flecainide and R-propafenone that act by reducing RyR2 inhibition [29,30].

Reperfusion changes the kinetics of sparks and increase the likelihood of Ca^{2+} waves—Even though ischemia is the triggering insult that activates electrical, metabolic and transcriptional changes in the heart, reperfusion after ischemia is the event that starts a functional “thunderstorm” that may lead to ventricular arrhythmias. The microscopic basis for this behavior can be extracted from data presented in Fig. 5A–D, where it is possible to observe the changes in the kinetics of the activation of Ca^{2+} sparks during reperfusion. Figs. 5B and 6A show a significant increase in the time to peak (Tp= 13.3 ±0.6 ms) with respect to ischemia. These results could suggest that the Ca^{2+} release through the RyR2 produced during a spark was maintained for a longer time during reperfusion. These changes in Ca^{2+} spark kinetics could be due to both an increase in the SR Ca^{2+} load and the re-establishment of the pH values [31]. Moreover, although Ca^{2+} sparks frequency displays a reduction during reperfusion vs. ischemia (Fig. 6D), there was a dramatic increase in the likelihood to develop Ca^{2+} waves (Fig. 5F–G and Fig. 6E). Fig. 5E shows a typical recording in which reperfusion drives an increase in the development of Ca^{2+} waves. Indeed, the probability of occurrence increased from 0.26 ± 0.03 waves/100μm/s (in the control condition) to 0.38 ± 0.04 waves/100μm/s during ischemia and 0.75 ± 0.15 waves/100μm/s during the reperfusion period (Fig. 6E). Figure S2 of online supplemental results is a typical movie showing Ca^{2+} waves during reperfusion in the whole heart. The fact that there was a decrease in Ca^{2+} spark frequency and an increase in the Ca^{2+} wave likelihood in reperfusion, suggests that the reduction in spark frequency is a consequence of the increase in waves. Furthermore, during reperfusion, the mechanisms that initiate spontaneous Ca^{2+} release seem to be increased and/or the mechanisms that are involved in the termination of spontaneous SR Ca^{2+} release were reduced. The increase in the likelihood of Ca^{2+} waves were mainly manifested at the onset of reperfusion, in a temporal association with the abrupt and transient increase in diastolic Ca^{2+} during reperfusion [4] and the initiation of arrhythmic electrical events, as we previously described [32]. Taken together, these results indicate that the spontaneous Ca^{2+} waves that break out with reperfusion, constitute a main substrate of the diastolic transient Ca^{2+} increase. These Ca^{2+} waves might also constitute the substrate of triggered arrhythmias at the onset of this period [33]. Indeed, the increase in wave incidence is an independent predictor of

arrhythmogenicity (i.e. it can predict the likelihood of Ca^{2+} waves to generate a delayed membrane depolarization (DAD) and triggered extrasystolic beats) [33–35].

Discussion

Myocardial infarction (MI) is a major cause of left ventricular dysfunction that leads to heart failure and arrhythmogenic sudden cardiac death in western nations [36]. Moreover, a hallmark of I/R injury is the alteration in Ca^{2+} homeostasis that occurs both, during ischemia and upon reperfusion. It is well established that this deregulated intracellular Ca^{2+} handling plays a major role in the pathophysiology of contractile, electrophysiological, and structural abnormalities that evolve after MI [37]. However, very little is known about the subcellular mechanisms responsible for these Ca^{2+} abnormalities.

Moreover, the assessment of Ca^{2+} spark properties at the intact heart level under physiological conditions (i.e. temperature, coronary perfusion, etc.) has been historically a big experimental challenge. The small amplitude of Ca^{2+} sparks limits the selection of fluorescent dyes to a few. The more typical dyes are fluorescein based such as Fluo-3 and Fluo-4 [26,27]. Unfortunately, these dyes can be efficiently extruded from ventricular cardiac myocytes through an adenosine binding cassette (ABC) protein. The protein, called multidrug resistant glycoprotein, hydrolyzes ATP to translocate an exogenous molecule like the dye, outside the cell [38]. This ATP hydrolytic dependency grants this transport system a high temperature dependence. Thus at 37°C, all the dye will be removed from the cell. This can be observed in Figure S3 of the online supplemental results, where Ca^{2+} transients were recorded with Fluo-4 by means of PLFFM. Figure S3A displays the time course of Ca^{2+} transients as the temperature of the heart was increased. Two clearly observed features are an increase in the velocity of Ca^{2+} transients and changes in the amplitude. Interestingly, if the heart was maintained at 37°C, the amplitude of the Ca^{2+} transients steadily diminished. This can be consistently observed in Figure S3B of online supplemental results, where the fluorescent signals reporting Ca^{2+} transients were significantly reduced after maintaining the heart for 20 min at 37°C. However, at 32°C, this transport system is highly impaired allowing us to perform the experiments at a temperature that, although not fully physiological, is still compatible with the mouse cardiac cycle within the physiological range. Furthermore, we demonstrated that the differences in kinetics between epi Ca^{2+} sparks and trabeculae Ca^{2+} sparks could be due to the fact that the overall Ca^{2+} signaling in the epicardium is faster than in endocardium. This increased speed of epi Ca^{2+} kinetics is a consequence of the increased level of RyR2 and SERCA2 at the epi layer in comparison with the endo layer. These molecular differences could also explain the differences between isolated myocyte (mostly derived from the endo region) Ca^{2+} sparks and epi whole heart Ca^{2+} sparks.

As a central aspect of the paper is to assess the diastolic Ca^{2+} signaling, confocal experiments were performed under a condition in which diastolic signaling is emphasized. Thus, not only ventricular Na^{+} channels were blocked by TTX but also the electrical conduction from the atrioventricular node to the purkinje fibers were slowed down by perfusing the heart with the muscarinic agonist, carbamylcholine. This pharmacological

maneuver expands the diastolic phase of the cardiac cycle and allowed us to increase the chance to observe Ca^{2+} sparks, a rather infrequent event at the whole heart level.

In addition, the model used in the present experiments allowed the exploration of the subcellular mechanism underlying Ca^{2+} homeostasis alterations in I/R in the intact heart. Furthermore, the present study made it possible to identify the subcellular events underlying two notable changes of the diastolic Ca^{2+} dynamics during I/R: First the increase in the diastolic Ca^{2+} during ischemia and second a “bump” like SR Ca^{2+} release at early time during reperfusion [4]. Thus, the two main conclusions of the present results, which confirm our initial hypothesis, are**: 1.** The increase in the frequency of diastolic Ca^{2+} sparks during ischemia is a major subcellular event underlying the increase of ischemia-induced diastolic Ca^{2+}. **2.** The increase in cytosolic Ca^{2+} waves are likely to be the main subcellular event underlying the abrupt diastolic Ca^{2+} rise at early times during reperfusion. The results further reveal the previously unrecognized main role of the SR in the increase in Ca^{2+} load during ischemia and proarrhythmogenic Ca^{2+} waves during reperfusion.

Ca^{2+} sparks are the substrate of ischemia-induced cytosolic Ca^{2+} overload during diastole

Ischemia represents a metabolic challenge to the heart that induces changes not only in diastole but also in systole. Certainly, we have already shown at the whole heart level, that an ischemic insult is able to modify the amplitude and kinetics of AP-induced Ca^{2+} transients and to produce an increase in both the cytosolic and intra SR diastolic Ca^{2+} levels [4,19]. The increase in cytosolic Ca^{2+} during ischemia has been mainly attributed to an enhanced Ca^{2+} influx through the Na^{+}-Ca^{2+} exchanger (NCX) and/or L-type Ca^{2+} channels [7,10]. Our results do not exclude any of these mechanisms but do emphasize the role of SR as a main effector of the ischemia-induced increase in cytosolic Ca^{2+}. The increase in the frequency of Ca^{2+} sparks observed during the ischemic period in our recordings, indicate that these events contribute to the ischemia-induced increase in diastolic Ca^{2+}. At first sight this may constitute an unexpected finding, owing to the fact that both SR Ca^{2+} uptake and release are impaired during ischemia, particularly due to the decrease in intracellular pH [31,39]. However, SR Ca^{2+} load increases during both, acidosis and ischemia [4,31]. This increase seems to be able to overcome the ischemia/acidosis-induced inhibitory effects on the Ca^{2+} handling proteins. Interestingly, the significantly higher frequency of Ca^{2+} sparks in ischemia, does not result in an increase of propagating Ca^{2+} waves relative to the preischemic period. A possible clue to explain these results may lie in the acidosis-induced decreased open probability of RyR2 channels in bilayers [31]. This action may oppose the Ca^{2+} overload effect of ischemia, breaking up cell-wide propagating waves into nonpropagating, spontaneous Ca^{2+} release events (wavelets or Ca^{2+} sparks), as described for other inhibitory RyR2 interventions [30].

Ca^{2+} waves: the underlying mechanism of reperfusion arrhythmias

Previous experiments of our labs have shown that the onset of reperfusion was associated with a large increase in cytosolic Ca^{2+} (Ca^{2+} bump), that originates at the SR level [4,31] and concurs with early reperfusion arrhythmias [32]. The present results extend these previous findings, by identifying the subcellular events that underlie the massive Ca^{2+} release that takes place upon reperfusion, i.e. Ca^{2+} sparks and, more important, Ca^{2+} waves.

Indeed, we found that the increase in the number of non-propagating events (Ca^{2+} sparks) observed in the ischemic period, converted into a significant increase in spontaneous propagating Ca^{2+} waves in reperfusion. This reduction in the Ca^{2+} spark frequency during reperfusion could be attributed to the fact that in presence of an increased Ca^{2+} wave frequency, the SR Ca^{2+} release machinery could be refractory to generate Ca^{2+} sparks. As previously discussed, experiments from our laboratory demonstrated that the open probability of RyR2 channels in bilayers increases when intracellular pH recovered after a period of acidosis [31], a situation that partially mimics the reperfusion condition. These findings strongly suggest that in contrast to ischemia, the increased open probability of RyR2 channels promotes first, an increase in the duration of Ca^{2+} sparks. These RyR2 channels, with a prolonged local Ca^{2+} release, would then be more prone to induce Ca^{2+} waves.

Abnormal intracellular Ca^{2+} cycling plays a key role in cardiac dysfunction and ventricular arrhythmias, particularly during the setting of transient cardiac ischemia followed by reperfusion. This is important in the clinical scenario as revealed by the numerous reports indicating a significant role for these arrhythmias either during spontaneous reperfusion after coronary spasms or after thrombolysis subsequent to acute myocardial infarction [40]. At the molecular level, the mechanisms of ventricular arrhythmias are heterogeneous, but common mechanisms have been identified in triggering arrhythmias as changes in the membrane potential, ion transporters, and altered intracellular Ca^{2+} handling. Ca^{2+} overload of the SR generates spontaneous release of Ca^{2+} through the RyR2 and a depolarizing inward current mediated by NCX. Indeed, a close association between spontaneous Ca^{2+}-oscillations, delayed after depolarizations (DADs) and reperfusion arrhythmias have been previously described [32,42]. These stimuli of non-reentry nature may give rise to episodes of ventricular tachycardia or fibrillation. Certainly, reperfusion arrhythmias usually lead to ventricular tachycardia that may degenerate in lethal ventricular fibrillation. Experimental evidence indicates that most of the ventricular tachycardia episodes leading to ventricular fibrillation at the onset of reperfusion, were initiated at the border of the reperfused zone by a non-reentrant mechanism and were maintained by both non-reentrant and reentrant mechanisms [41,42]. Moreover, it has been previously stated that the increase in Ca^{2+} wave incidence is an independent predictor of the likelihood of Ca^{2+} waves to generate a DAD and triggered beats [33–35]. In the present work, we showed an enhanced incidence of Ca^{2+} waves during reperfusion. This finding would indicate that Ca^{2+} waves constitute a main subcellular precursor of triggered arrhythmias upon reperfusion.

Conclusions

Using whole heart confocal microscopy, the present results assessed Ca^{2+} sparks at the intact heart level for the first time. This approach allows us to establish a new paradigm relative to the mechanisms underlying the increase in cytosolic Ca^{2+} in I/R, i.e. the results revealed that **1.** An increase in the frequency of Ca^{2+} sparks and waves, are main microscopic events underlying the increase in diastolic Ca^{2+} during ischemia and the likelihood of reperfusion arrhythmias. **2.** The SR Ca^{2+} overload plays a previously unrecognized key role in the underlying mechanisms of Ca^{2+} mishandling in I/R, being the final responsible for the ischemia-induced increase in Ca^{2+} sparks and reperfusion Ca^{2+}

waves. The results thus provide subcellular basis for a better comprehension of the alterations in Ca^{2+} homeostasis that occur in I/R and can contribute to initiate triggered reperfusion arrhythmias.

Potential clinical implications and limitations of the study

MI is a main cause of left ventricular dysfunction leading to heart failure, ventricular arrhythmias and sudden death. A major challenge to prevent these life threatening complications is the recognition of their underlying mechanisms. In the present study we demonstrated that an increase in Ca^{2+} sparks and waves are the microscopic events of Ca^{2+} overload and proarrhythmogenic events in ischemia and reperfusion, respectively. The results also emphasize the crucial role of the SR in I/R Ca^{2+} overload. We are aware however, of the limitations of any animal model to mimicking MI in patients and therefore extrapolation of our findings to the clinical setting should be very cautious. Moreover, the mechanistic link between MI, cardiac arrhythmias and reperfusion-induced Ca^{2+} waves in patients is unknown and requires extensive work in subsequent studies.

As a down side of our experimental approach, changes in the metabolism during deep bradycardia and alterations in Na^{+} influx by TTX could distort the clinical scenario present during a real infarction. It has been reported that TTX can reduce intracellular Na^{+} concentration [43], a situation that may protect from increases in intracellular diastolic $[Ca^{2+}]$ and $[H^{+}]$ and therefore would tend to decrease the magnitude of our already significant results. Moreover, ischemia promotes an initial ventricular bradycardia [44]. Taken together these considerations, we think that our experimental conditions would not significantly diverge from a real infarction.

Furthermore, our model allows measurements of subcellular Ca^{2+} sparks and waves at the epicardial layer of the heart which may be not fully representative of whole heart behavior. Nevertheless, our approach allowed a clear characterization in the intact heart of the submicroscopic events that take place during I/R and are the substrates of Ischemia-induced Ca^{2+} load and arrhythmogenic reperfusion Ca^{2+} waves.

Although the hearts have been pharmacologically immobilized, it is very difficult to prevent sub-micrometer movements that will mask the Ca^{2+} kinetics and activity. This experimental constrain prevented us to directly perform experiments measuring the electrical behavior simultaneously with the subcellular Ca^{2+} dynamics at the intact heart level. Further experimental and translational studies are needed to evaluate the possibility that the increase in Ca^{2+} waves here described upon reperfusion are the substrate of reperfusion arrhythmias in the clinical scenario.

Finally, the focus of our work was to elucidate the subcellular mechanisms underlying the macroscopic anomalous Ca^{2+} dynamics during I/R, previously described [4]. We are aware of the fact that multiple possible complex processes (CaMKII activation, ROS signaling, etc.) may be involved in the genesis of this new pathophysiological paradigm, i.e. the increase in Ca^{2+} sparks during ischemia that reperfusion transforms in arrhythmogenic events. Future experiments along these lines will be performed in our laboratories to further elucidate the complex I/R setting.

Supplementary Material

Refer to Web version on PubMed Central for supplementary material.

Acknowledgments

Sources of Funding

This work was supported by NIH grants R01-HL-084487(to ALE), PIP 0890 (CONICET) to AM and PICT 1903 (FONCYT) (to AM and ALE).

We deeply thank Dr. Laura Borodinsky from UC Davis for the use of their vibratome.

References

1. Marban E, Kitakaze M, Kusuoka H, Porterfield JK, Yue DT, Chacko VP. Intracellular free calcium concentration measured with 19F NMR spectroscopy in intact ferret hearts. Proc Natl Acad Sci USA. 1987; 84:6005–6009. [PubMed: 3112778]
2. Miyamae M, Camacho SA, Weiner MW, Figueredo VM. Attenuation of postischemic reperfusion injury is related to prevention of [Ca2+]m overload in rat hearts. Am J Physiol. 1996; 271:H2145–H2153. [PubMed: 8945935]
3. Ruiz-Meana M, Garcia-Dorado D, Julia M, et al. Protective effect of HOE642, a selective blocker of Na^+-H^+ exchange, against the development of rigor contracture in rat ventricular myocytes. Exp Physiol. 2000; 85:17–25. [PubMed: 10662888]
4. Valverde CA, Kornyeyev D, Ferreiro M, Petrosky AD, Mattiazzi A, Escobar AL. Transient Ca^{2+} depletion of the sarcoplasmic reticulum at the onset of reperfusion. Cardiovasc Res. 2010; 85:671–680. [PubMed: 19920131]
5. Pike MM, Kitakaze M, Marban E. 23Na-NMR measurements of intracellular sodium in intact perfused ferret hearts during ischemia and reperfusion. Am J Physiol. 1990; 259:H1767–H1773. [PubMed: 2260701]
6. Inserte J, Barba I, Hernando V, Garcia-Dorado D. Delayed recovery of intracellular acidosis during reperfusion prevents calpain activation and determines protection in postconditioned myocardium. Cardiovasc Res. 2009; 81:116–122. [PubMed: 18829701]
7. Murphy E, Perlman M, London RE, Steenbergen C. Amiloride delays the ischemia-induced rise in cytosolic free calcium. Circ Res. 1991; 68:1250–1258. [PubMed: 1902148]
8. Ten Hove M, Nederhoff MG, Van Echteld CJ. Relative contributions of Na^+/H^+ exchange and Na^+/HCO_3^- cotransport to ischemic Na_i^+ overload in isolated rat hearts. Am J Physiol Heart Circ Physiol. 2005; 288:H287–H292. [PubMed: 15319198]
9. Ten Hove M, Jansen MA, Nederhoff MG, van Echteld CJ. Combined blockade of the Na+ channel and the Na+/H+ exchanger virtually prevents ischemic Na^+ overload in rat hearts. Mol Cell Biochem. 2007; 297:101–110. [PubMed: 17102905]
10. Sun J, Picht E, Ginsburg KS, Bers DM, Steenbergen C, Murphy E. Hypercontractile female hearts exhibit increased S-nitrosylation of the L-type Ca^{2+} channel alpha1 subunit and reduced ischemia/reperfusion injury. Circ Res. 2006; 98:403–411. [PubMed: 16397145]
11. Neely JR, Rovetto MJ, Whitmer JT, Morgan HE. Effects of ischemia on function and metabolism of the isolated working rat heart. Am J Physiol. 1973; 225:651–658. [PubMed: 4726499]
12. Steenbergen C, Perlman ME, London RE, Murphy E. Mechanism of preconditioning. Ionic alterations. Circ Res. 1993; 72:112–125. [PubMed: 8380259]
13. Kass RS, Tsien RW. Fluctuations in membrane current driven by intracellular calcium in cardiac purkinje fibers. Biophys J. 1982; 38:259–269. [PubMed: 6809065]
14. Marban E, Robinson SW, Wier WG. Mechanisms of arrhythmogenic delayed and early afterdepolarizations in ferret ventricular muscle. J Clin Invest. 1986; 78:1185–1192. [PubMed: 3771791]

15. Kusuoka H, Porterfield JK, Weisman HF, Weisfeldt ML, Marban E. Pathophysiology and pathogenesis of stunned myocardium. Depressed Ca^{2+} activation of contractionas a consequence of reperfusion-induced cellular calcium overload inferret hearts. J Clin Invest. 1987; 79:950–961. [PubMed: 3818956]
16. Piper HM, Abdallah Y, Schafer C. The first minutes of reperfusion: a window of opportunity for cardioprotection. Cardiovasc Res. 2004; 61:365–371. [PubMed: 14962469]
17. Dou Y, Arlock P, Arner A. Blebbistatin specifically inhibits actin-myosin interaction in mouse cardiac muscle. Am J Cell Physiol. 2007; 293:C1148–1153.
18. Ferreiro M, Petrosky AD, Escobar AL. Intracellular Ca2+ release underlies the development of phase 2 in mouse ventricular action potentials. Am J Physiol Heart Circ Physiol. 2012; 302(5):H1160–72. [PubMed: 22198177]
19. Valverde CA, Mundiña-Weilenmann C, Reyes M, Kranias EG, Escobar AL, Mattiazzi A. Phospholamban phosphorylation sites enhance the recovery of intracellular Ca^{2+} after perfusion arrest in isolated, perfused mouse heart. Cardiovasc Res. 2006; 70:335–345. [PubMed: 16516179]
20. Mejía-Alvarez R, Manno C, Villalba-Galea CA, Fernández LDV, Ribeiro Costa R, Fill M, et al. Pulsed local-field fluorescence microscopy: a new approach for measuring cellular signals in the beating heart. Pfluger Arch. 2002; 445(6):747–58.
21. McManus OB, Blatz AL, Magleby KL. Sampling, log binning, fitting, and plotting durations of open and shut intervals from single channels and the effects of noise. Pflugers Arch. 1987; 410:530–53. [PubMed: 2448743]
22. Sigworth FJ, Sine SM. Data transformations for improved display and fitting of single-channel dwell time histograms. Biophys J. 1987; 52:1047–1054. [PubMed: 2447968]
23. Wier WG, ter Keurs HE, Marban E, Gao WD, Balke CW. Ca2+ ‘sparks’ and waves in intact ventricular muscle resolved by confocal imaging. Circ Res. 1997; 81:462–469. [PubMed: 9314826]
24. Boyett MR. Effect of rate-dependent changes in the transient outward current on the action potential in sheep Purkinje fibres. J Physiol. 1981; 319:23–41. [PubMed: 7320913]
25. Litovsky SH, Antzelevitch C. Transient outward current prominent in canine ventricular epicardium but not endocardium. Circ Res. 1988; 62(1):116–26. [PubMed: 2826039]
26. Cheng H, Lederer WJ, Cannell MB. Calcium sparks: elementary events underlying excitation-contraction coupling in heart muscle. Science. 1993; 262:740–744. [PubMed: 8235594]
27. Kockskämper J, Sheehan KA, Bare DJ, Lipsius SL, Mignery GA, Blatter LA. Activation and propagation of Ca(2+) release during excitation-contraction coupling in atrial myocytes. Biophys J. 2001; 81:2590–2605. [PubMed: 11606273]
28. Escobar AL, Perez CG, Reyes ME, et al. Role of Inositol-1, 4, 5-Trisphosphate in the Regulation of Ventricular Ca^{2+} Signaling in IntactMouse Heart. J Mol Cell Cardiol. 2012; 3(6):768–79. [PubMed: 22960455]
29. Hilliard FA, Steele DS, Laver D, et al. Flecainide inhibits arrhythmogenic Ca^{2+} waves by open state block of ryanodine receptor Ca^{2+} release channels and reduction of Ca^{2+} spark mass. J Mol Cell Cardiol. 2010; 48:293–301. [PubMed: 19835880]
30. Galimberti ES, Knollmann BC. Efficacy and potency of class I antiarrhythmic drugs for suppression of Ca^{2+} waves in permeabilized myocytes lacking calsequestrin. J Mol Cell Cardiol. 2011; 51:760–768. [PubMed: 21798265]
31. Said M, Becerra R, Palomeque J, et al. Increased intracellular Ca^{2+} and SR Ca^{2+} load contribute to arrhythmias after acidosis in rat heart. Role of Ca2+/calmodulin-dependent protein kinase II. Am J Physiol Heart Circ Physiol. 2008; 295:H1669–H1683. [PubMed: 18723772]
32. Said M, Becerra R, Valverde CA, et al. Calcium-calmodulin dependent protein kinase II (CaMKII): a main signal responsible for early reperfusion arrhythmias. J Mol Cell Cardiol. 2011; 51:936–44. [PubMed: 21888910]
33. Takamatsu T, Wier WG. Calcium waves in mammalian heart: quantification of origin, magnitude, waveform, and velocity. FASEB J. 1990; 4:1519–1525. [PubMed: 2307330]
34. Cheng H, Lederer MR, Lederer WJ, Cannell MB. Calcium sparks and $[Ca^{2+}]_i$ waves in cardiac myocytes. Am J Physiol. 1996; 270:C148–C159. [PubMed: 8772440]

35. Kubalova Z, Gyorke I, Terentyeva R, et al. Modulation of cytosolic and intra-sarcoplasmic reticulum calcium waves by calsequestrin in rat cardiac myocytes. J Physiol. 2004; 561:515–524. [PubMed: 15486014]
36. Lloyd-Jones D, Adams R, Carnethon M, et al. Heart disease and stroke statistics—2009 update: a report from the American Heart Association Statistics Committee and Stroke Statistics Subcommittee. Circulation. 2009; 119:e181.
37. Gomez AM, Guatimosim S, Dilly KW, Vassort G, Lederer WJ. Heart failure after myocardial infarction: altered excitation-contraction coupling. Circulation. 2001; 104:688–693. [PubMed: 11489776]
38. Di Virgilio F, Steinberg TH, Swanson JA, Silverstein SC. Fura-2 secretion and sequestration in macrophages. A blocker of organic anion transport reveals that these processes occur via a membrane transport system for organic anions. J Immunol. 1988; 140:915–920. [PubMed: 3339244]
39. Mandel F, Kranias EG, Grassi de Gende A, Sumida M, Schwartz A. The effect of pH on the transient-state kinetics of Ca^{2+}-Mg^{2+}-ATPase of cardiac sarcoplasmic reticulum. A comparison with skeletal sarcoplasmic reticulum. Circ Res. 1982; 50:310–317. [PubMed: 6120049]
40. Salerno JA, Previtali M, Chimienti M, Klersy C, Bobba P. Vasospasm and ventricular arrhythmias. Ann N Y Acad Sci. 1984; 427:222–233. [PubMed: 6588895]
41. Lakireddy V, Bub G, Baweja P, Syed A, Boutjdir M, El-Sherif N. The kinetics of spontaneous calcium oscillations and arrhythmogenesis in the in vivo heart during ischemia/reperfusion. Heart Rhythm. 2006; 3:58–66. [PubMed: 16399055]
42. Pogwizd SM, Corr PB. Electrophysiologic mechanisms underlying arrhythmias due to reperfusion of ischemic myocardium. Circulation. 1987; 72:404–26. [PubMed: 3608126]
43. Saint DA. The role of the persistent Na(+) current during cardiac ischemia and hypoxia. J Cardiovasc Electrophysiol. 2006; 17(Suppl 1):S96–S103. [PubMed: 16686689]
44. Pentecost BL, Bennett MA, George CF. Bradyarrhythmia complicating myocardial infarction. Lancet. 1968; 2:1300–1. [PubMed: 4177501]

Highlights

- Ca^{2+} sparks were assessed and characterized for the first time in the whole heart.
- Ca^{2+} sparks frequency increase during ischemia is a substrate for Ca^{2+} overload.
- Early diastolic Ca^{2+} rise during reperfusion is mediated by Ca^{2+} waves.

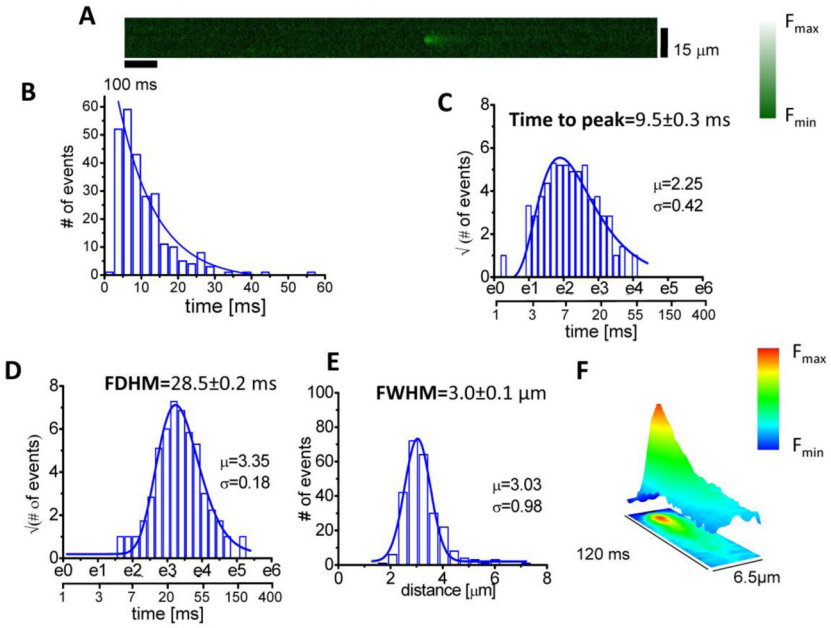

Figure 1. Characteristics of epi Ca^{2+} sparks in the intact heart

A. Typical example of a line-scan-recording of epi Ca^{2+} sparks obtained in the intact heart. **B.** Linear binned distribution of time to peak (Tpeak). **C.** Log binned distribution of Tpeak. Note that e is the base of natural logarithm, e= 2.718281828. So, e^n is 2.718281828^n. **D.** Full duration at half maximum (FDHM) and E. Full width at half maximum (FWHM) of Ca^{2+} sparks in the intact heart at 32°C. Data are mean of 573 events from 6 different hearts. **F.** x-t plot of an average of 10 sparks.

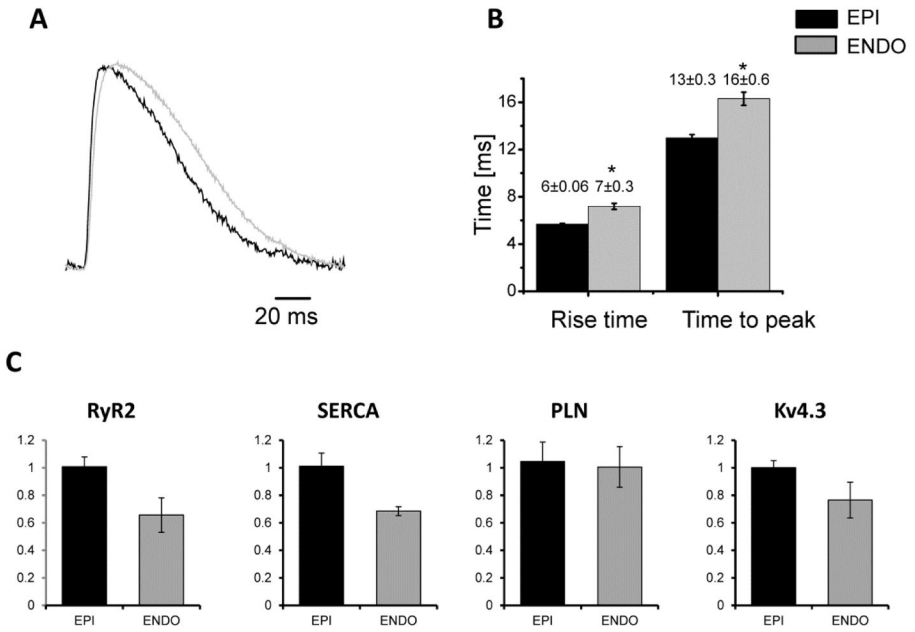

Figure 2. Functional and mRNA differences across the ventricular wall

A. Typical records of Ca^{2+} transients obtained in the epi and endo layer of the ventricular wall. **B** Overall results of 6 experiments. **C to D**. Average results of mRNA of RyR2, SERCA2, PLN and Kv4.3 in endo and epi. Data and mean ± SEM of 5 experiments. *P<0.05.

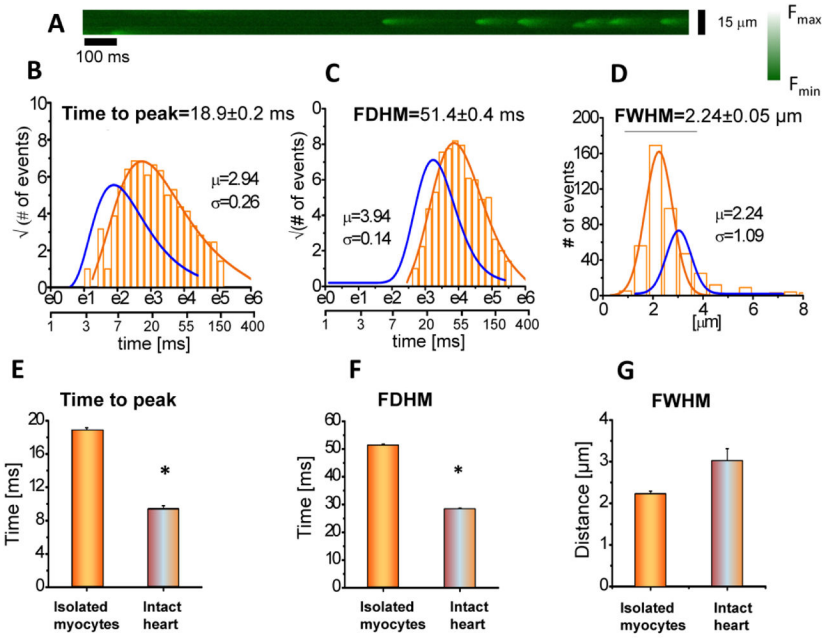

Figure 3. Ca^{2+} sparks in the intact heart are faster than sparks in isolated cells

A. Typical example of a line-scan-recording of Ca^{2+} sparks obtained in isolated ventricular myocytes at 32°C. **B to D**: Distribution of time to peak (Tpeak), full duration at half maximum (FDHM) and full width at half maximum (FWHM) of Ca^{2+} sparks in isolated myocytes at 32°C. Superimposed in blue are the results obtained in the intact heart, showed in Figure 1, to facilitate comparison. Data are the results of 19 cells from 5 hearts. **E to G**. Time to peak and the full duration at half maximum (FDHM) were significantly shorter in the intact heart than in the isolated myocytes, whereas the full width at half maximum (FWHM) was significantly larger. Data are mean ± SEM of 573 events from 6 different hearts and 19 isolated myocytes. *P<0.05.

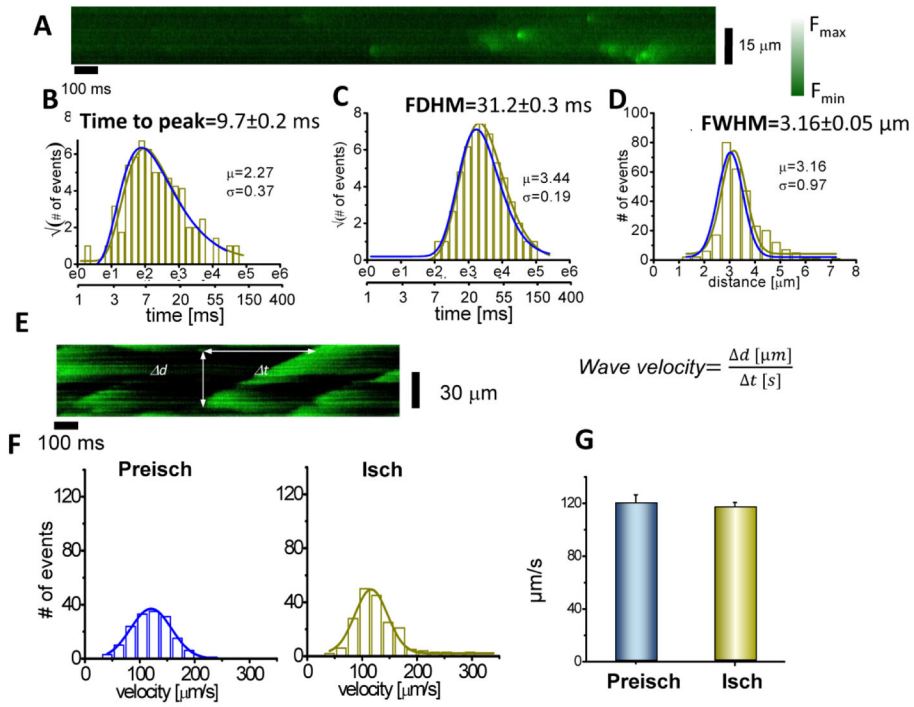

Figure 4. Ca^{2+}spark and waves are similar in ischemia and in preischemia

A. Typical example of a line-scan-recording of epi Ca^{2+} sparks obtained in the intact heart during ischemia. **B to D:** Distribution of time to peak (Tpeak), full duration at half maximum (FDHM) and full width at half maximum (FWHM) of Ca^{2+} sparks in the intact heart during ischemia. Superimposed in blue are the results obtained during preischemia, showed in Figure 2, for a better comparison. Data are mean of 513 events from 6 different hearts. E. x-t plot of an average of 10 sparks. **E.** Typical example of a line-scan-recording of epi Ca^{2+} waves obtained in the intact heart during ischemia. It also illustrates the method used to calculate the velocity of Ca^{2+}waves. **F to G.** Distribution and mean velocity of Ca^{2+}waves, during preischemia and ischemia in the intact heart, respectively. No differences were observed in any of these parameters between preischemia and ischemia. Data are obtained from the analysis of 118 and 238 waves in preischemia and ischemia respectively, from 6 different hearts.

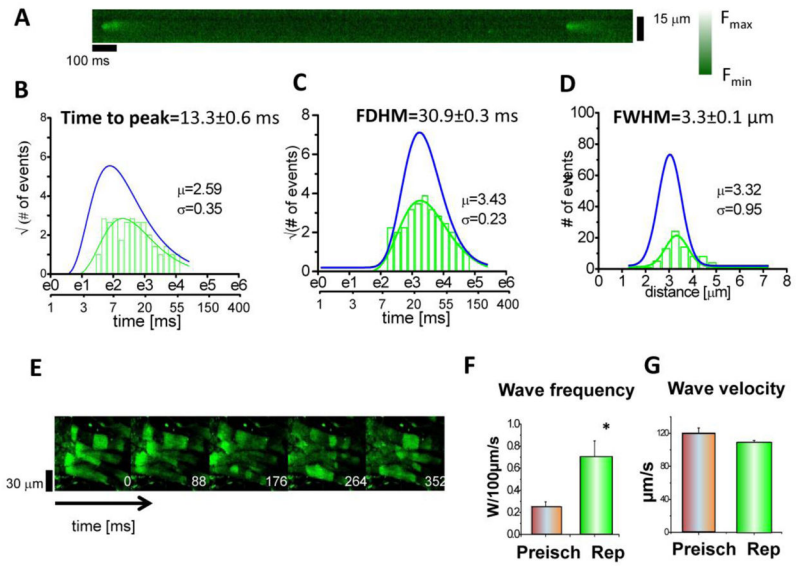

Figure 5. Reperfusion decreases Ca^{2+} spark frequency, changes Ca^{2+} spark dynamic and increases the frequency of Ca^{2+}waves, relative to ischemia

A. Typical example of a line-scan-recording of Ca^{2+} sparks during the reperfusion period in the intact heart. **B to D:** Distribution of Time to peak (Tpeak), full duration at half maximum (FDHM) and full width at half maximum (FWHM) of epi Ca^{2+} sparks in the perfused intact heart. Superimposed in blue are the results obtained during ischemia, showed in Figure 4, to facilitate comparison. Data are mean of 118 events from 5 different hearts. E. x-t plot of an average of 10 sparks. **E:** Typical example of a line-scan-recording of epi Ca^{2+}waves obtained in the intact heart during ischemia. **F and G:** Overall results depicting the significant increase in the frequency of Ca^{2+} waves (**F**) and the lack of changes in wave velocity (**G**) in reperfusion vs. preischemia. Data are mean of 163 events from 5 different hearts

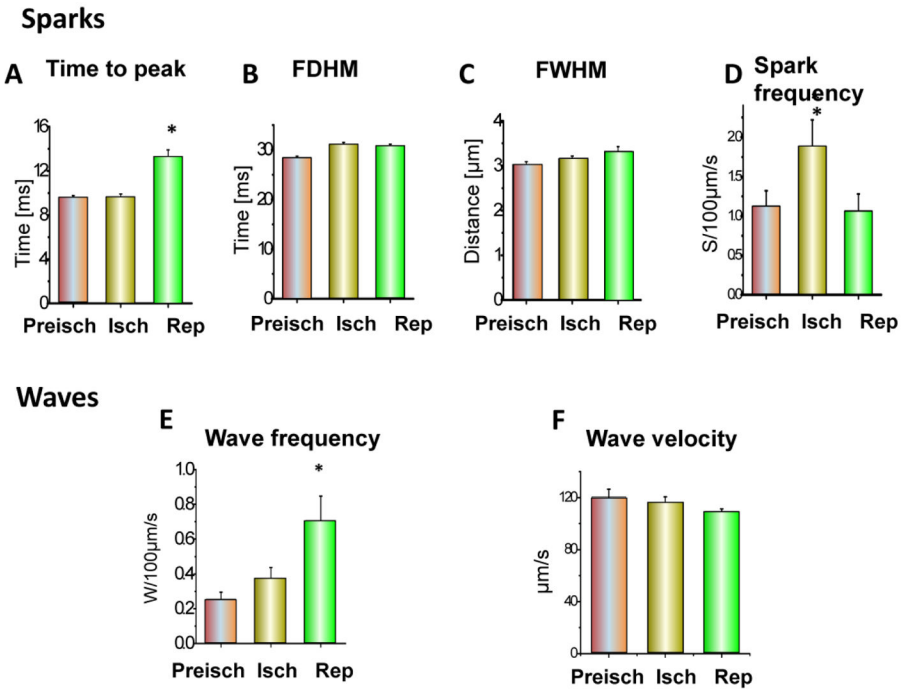

Figure 6. Summary of the characteristics of Ca^{2+}sparks and waves in the intact heart during preischemia, ischemia and reperfusion

A to D: Reperfusion increased time to peak with respect to preischemia and ischemia. Additionally, the likelihood of Ca^{2+}sparks increased during ischemia with respect to preischemia. Mean ± SEM of 573, 513 and 163 events from 5–6 different hearts in preischemia, ischemia and reperfusion, respectively, in the intact heart. **E to F:** Reperfusion increased wave frequency vs. ischemia and preischemia (**E**), but did not affect wave velocity (**F**). Data represent Mean ± SEM of 118, 238 and 502 events from 5–6 different hearts in preischemia (PI), ischemia (I) and reperfusion (R), respectively. *P<0.05 vs. preischemia and ischemia.